Does string fragmentation reveal more than longitudinal phase space?

H. J. Schulze and J. Aichelin
Institut für Theoretische Physik der Universität Heidelberg and Max-Planck-Institut für Kernphysik, D-6900 Heidelberg, Germany
(Received 28 November 1988)

The fragmentation of a color string into hadrons is assumed to be a sequence of binary decays governed by Fermi's golden rule. In each decay step a hadron is produced and a string with lower energy is left. Assuming that the transition matrix element depends on p_T only the decay is completely determined by the longitudinal phase space and one parameter, the $\langle p_T^2 \rangle$ of the produced hadrons. We find an almost complete agreement with the experimental momentum (longitudinal and transversal) and multiplicity distributions and the number of produced particles. The "seagull" shape of $\langle p_T^2 \rangle(x)$ turns out to be completely due to the sphericity analysis. This leaves little room for extracting information of QCD from single-particle-inclusive fragmentation data.

The fragmentation of color strings produced in e^+e^-, μp, and pp collisions shows striking similarities. This suggests a common fragmentation mechanism. The first mechanism proposed was the longitudinal-phase-space dominance.[1] Later, more involved models were developed, which combined assumptions about the QCD matrix elements (in terms of fragmentation functions and branching ratios) with the longitudinal phase space. We mention the Field-Feynman,[2] Lund,[3] and Webber,[4] models. Generally these models contain quite a few parameters which are adjusted by comparison with data. They have in common an almost complete agreement with experiment in spite of vastly different basic assumptions.

We think it is premature to discuss whether string fragmentation reveals information about QCD before one has investigated in detail the final-state distribution expected from a decay which is completely governed by phase space. There are two scenarios which one can imagine to be completely phase-space dominated: Either an instantaneous production of all final-state hadrons or a sequential binary decay where in each step a hadron is emitted and a string with lower energy is left, analogous to the decay of a compound nucleus. Both processes yield quite different results for the number of produced particles and their momentum spectra. The first process was recently investigated by Kurihara, Hüfner, and Aichelin.[5] In this article we explore the second approach. We assume—as did Field-Feynman and the Lund group—that string fragmentation is a sequence of binary decays where in the ith step a string of invariant mass M_{i-1} decays into a hadron of species m_i and a string of mass M_i:

$$\underbrace{\text{string}(M_{i-1})}_{i} \rightarrow \underbrace{\text{string}(M_i)+\text{hadron}(m_i)}_{f} . \tag{1}$$

The sequence starts with $M_0=\sqrt{s}$ and terminates when there is no energy left in the string. The decay rate for each step in the rest system of the string is given by Fermi's golden rule:

$$\Gamma_{i-1,i}(M_{i-1}\rightarrow M_i+m_i)=\int \frac{d^4P_i d^4p_i}{(2\pi)^8}|T_{if}(P_i,p_i)|^2 . \tag{2}$$

Defining

$$|T_{i-1,i}(P,p)|^2 \equiv 2(2\pi)^8 f_{Mm}(y,\mathbf{p}_T) \times \delta(p^2-m^2)\Theta(p_0)\delta^4(P_{i-1}-P-p) , \tag{3}$$

we obtain

$$\Gamma_{i-1,i}=\int dy\, d^2\mathbf{p}_T f_{Mm}(y,\mathbf{p}_T) ; \tag{4}$$

i.e., f is the fragmentation function for the emission of a hadron m with rapidity y and transverse momentum $\mathbf{p}_T$ from the string M. We assume that in longitudinal direction string fragmentation is determined by phase space:

$$f_{Mm}(y,\mathbf{p}_T)=C_M S_m \Theta(M/2-m_T\cosh y)e^{-p_T^2/\lambda} , \tag{5}$$

where C_M is a constant, $S_m=(2J_m+1)(2I_m+1)$, the Θ function expresses energy conservation, and λ is a free parameter. It is taken as 0.8 $(\text{GeV}/c)^2$ in order to give best agreement with experiments. If we neglect the kinematical bound for $p_T(y)$, we get for the longitudinal fragmentation function

$$\frac{dN_{Mm}}{dy} \equiv \int d^2\mathbf{p}_T f_{Mm}(y,\mathbf{p}_T) \approx C'_M S_m \Theta(y_{\max}(M,m)-|y|) , \tag{6}$$

with

$$y_{\max}(M,m)=\operatorname{arccosh}\left[\frac{M/2}{m}\right] . \tag{7}$$

λ is the only parameter used so far. However, there is a hidden parameter, the number of species of hadrons which we allow to be produced. For the mesons it turns out that the final hadron distribution (charged pions and kaons) is almost independent of the resonances included. The baryon-to-meson ratio, however, depends on the ratio of mesonic and baryonic resonances included, provided one assumes a common transition matrix element

$|T_{if}|^2$.

Before we proceed to the detailed numerical calculation it is advised to start with some analytical results. For this purpose we neglect the recoil momentum of the string and assume only one species of decay products with a constant $p_T = \langle p_T \rangle$. The fragmentation function is then

$$\frac{dN_{Mm}}{dy} = \frac{1}{2y_{\max}(M,m)} \Theta(y_{\max}(M,m) - |y|) \tag{8}$$

and the average energy of the emitted hadron is

$$\langle E \rangle = \int_{-y_{\max}}^{+y_{\max}} dy \frac{dN}{dy}(y) E(y) = \frac{1}{y_{\max}} p_L(y) \Big|_0^{y_{\max}} = \frac{p_{L\max}}{y_{\max}} , \tag{9}$$

where M is the mass of the string prior to fragmentation. Replacing the logarithmic dependence of $y_{\max}$ on the string energy M by a constant $\tilde{y}$ and neglecting terms of the order (m_T^2/M^2), we obtain, for the average energy loss of the string,

$$\langle M_{i-1} - M_i \rangle = \langle E_i \rangle \approx \frac{M_{i-1}}{2\tilde{y}} . \tag{10}$$

After i decay steps, the mass of the string is

$$M_i = M_0 \left[1 - \frac{1}{2\tilde{y}} \right]^i \approx M_0 e^{-i/2\tilde{y}} . \tag{11}$$

The average number of hadrons produced in the decay of a string with the initial energy M_0 can be obtained requiring the decay terminates when $M_i \leq m_T$:

$$\langle N \rangle (M_0) = 2\tilde{y} \ln \left[\frac{M_0}{m_T} \right] . \tag{12}$$

The fragmentation function follows immediately from Eq. (8). We neglect again the logarithmic dependence of the normalization on the string energy and obtain

$$\begin{aligned} \frac{dN_i}{dy} &= \frac{1}{2y_{\max}(M_{i-1})} \Theta(y_{\max}(M_{i-1}) - |y|) \\ &\approx \frac{1}{2\tilde{y}} \Theta(y_{\max}(M_{i-1}) - |y|) , \\ \frac{dN}{dy}(y) &= \sum_{i=1}^{i_{\max}(y)} \frac{dN_i}{dy}(y) \approx i_{\max}(y) \frac{1}{2\tilde{y}} \\ &\approx \ln \left[\frac{M_0}{2E(y)} \right] . \end{aligned} \tag{13}$$

Introducing the Feynman variable $x = 2p_L/M_0$ it follows that

$$\begin{aligned} \frac{dN_{\text{ch}}}{dx}(x) &= \frac{2}{3} \left[\frac{M_0}{2E(x)} \right] \ln \left[\frac{M_0}{2E(x)} \right] \\ &= -\frac{2}{3} \frac{\ln[x^2 + (2m_T/\sqrt{s})^2]^{1/2}}{[x^2 + (2m_T/\sqrt{s})^2]^{1/2}} , \end{aligned} \tag{14}$$

because only $\frac{2}{3}$ of the particles are charged. Please note that the $\tilde{y}$'s cancel and therefore the fragmentation function is completely determined once $\langle p_T \rangle$ is chosen. There is no other parameter. Scaling is violated at low x by the factor $[x^2 + (2m_T/\sqrt{s})^2]^{1/2}$, in agreement with European Muon Collaboration data and Ref. 5. For low x the results of this simplified analytical model agree not only qualitatively but even quantitatively with data as can be seen in Fig. 1. This indicates that the results are essentially determined once $\langle p_T \rangle$ is chosen and the extension to different species does only change the finer de-

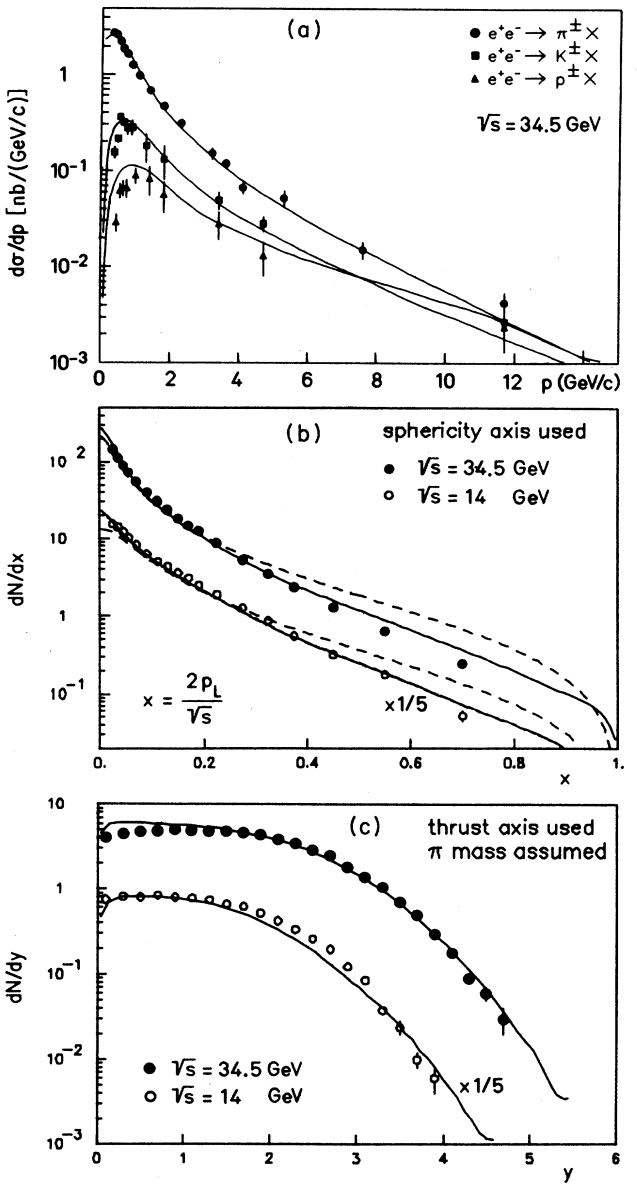

FIG. 1. Momentum distributions. (a) shows the distribution of $|\mathbf{p}|$ separately for charged pions, kaons, and (anti)protons at $\sqrt{s} = 34.5$ GeV. (b) and (c) show the distributions of $x_L = p_L/(\sqrt{s}/2)$ and rapidity y at 14 GeV (○) and 34.5 GeV (●). The result of the simplified calculation Eq. (14) is displayed as a dashed line.

tails of the distribution.

We proceed now to the detailed calculation, which is performed employing a Monte Carlo method. During the decay we allow the production of

$$m = \begin{cases} \pi,\eta,\eta',K,D,D_s,B,B_s,\rho,\phi,\omega,K^*,D^*,D_s^*,B^*,B_s^* \\ (\text{mesons}) , \\ N,\Lambda,\Sigma,\Xi \quad (\text{baryons}) , \end{cases}$$

with the momentum distributions

$$\frac{dN_{Mm}}{dy} = \text{const} = \frac{1}{2y_{\max}} \Theta(y_{\max} - |y|) ,$$
$$\frac{dN_{Mm}}{dp_T^2}\bigg|_y \sim e^{-p_T^2/\lambda} \Theta\left(\frac{M}{2} - E(y,\mathbf{p}_T)\right) . \tag{15}$$

We generated 100 000 two-jet events at string energies of 34.5 and 14 GeV to allow comparison with TASSO data.[6] Flavor and baryon number are conserved in the string by requiring that baryon and antibaryon, and the flavor partners of the mesons are created in pairs. The only exception is the first step where we assume that an open strange, charm, or bottom meson is produced according to the kind of the string ($d\bar{d}:u\bar{u}:s\bar{s}:c\bar{c}:b\bar{b} = 1:4:1:4:1$). Once the primary hadron is emitted with four-momentum $p = (m_T \cosh y,\ m_T \sinh y,\ \mathbf{p}_T)$, four-momentum conservation is provided by adding the recoil $-p$ to the (anti)quark on the same "side" of the string. Then the new string energy M_i and the Lorentz transformation matrix Λ_i (consisting of a boost and a rotation) to the c.m. system of the new string are computed and the decay resumes in this new Lorentz frame. This procedure continues until the string energy M_i is smaller than the pion mass.

The primary produced hadrons are usually short lived and decay into "stable" final-state particles π, K, and N. We have implemented all the experimentally known decay channels with decay fractions of more than about five percent. All the two-, three-, and four-body decays are generated as phase-space decays. Since the decay channels and absolute fractions of the D and B mesons are partly very poorly known, this introduces some uncertainty to our model. The influence of these uncertainties we have checked by replacing the known B decays by a pure phase-space decay into pions. The resulting changes are very small as far as the observed particles are concerned. The influence on the number of resonances is hard to be estimated.

To compare with experimental data, sphericity and thrust axis are computed and multiplicity distributions, inclusive momentum distributions of charged particles with respect to these axes, etc., are recorded.

Figure 1 shows momentum distributions of the produced hadrons. In Fig. 1(a) we present the calculated distribution in $p = |\mathbf{p}|$ for π, K, and p separately as compared to the data of Ref. 6. We see an increase of the distribution at low momentum and a decrease at high momentum. As also seen experimentally, the momentum at the maximum of the calculated distribution is different for the different species. It is determined by the scale-breaking term of Eq. (14). We observe a good agreement between theory and experiment for the absolute yield as well as for the shape. The relative ratio of pions, kaons, and protons is only due to the different masses of these particles and the primordial resonances which produce them. No additional suppression factor is required. Figures 1(b) and 1(c) display the momentum distribution of all charged hadrons for two different energies (14 and 34.5 GeV). In Fig. 1(b) the distribution is plotted as a function of Feynman x ($x = 2p_L/\sqrt{s}$). At large x the distribution is a function of x only; at low x we observe a scale breaking (i.e., a dependence of the distribution on the energy of the string), as predicted already by Eq. (14). The distribution obtained in our simplified model (with $m_T = 0.4$ GeV) Eq. (14) is displayed as dashed lines. It agrees quite well with the more sophisticated calculation at low x but differs at large x. This difference is due to the formation of resonances. Resonances have a higher mass compared to the observed particles and therefore their maximum momentum for a given string energy is lower. This depopulates the large-x region. It is not completely counterbalanced by the resonance decay because on the average only $\frac{1}{3}$ of the momentum is in the direction of the jet. Hence the decay products do not populate the large-x region in the same way as one would observe for a decay of the string into pions only. The rapidity distribution is displayed in Fig. 1(c). Both the x and the rapidity distribution agree quite well with data. We observe a plateau in the central rapidity region whose extension increases with beam energy.

Figure 2(a) shows the multiplicity distribution of the primordial hadrons as compared with that of the observed particles. We see that only a small fraction of the observed pions is directly produced. Most of them come from resonance decay. This questions the applicability of pion interferometry to determine the source size. Please note that the ratio between strange and nonstrange particles, which is also determined by phase space only, is reproduced quite well. We also find a good agreement between theory and data for high-mass resonances such as ρ_0 and K^* despite the poor knowledge of their production in B- and D-meson decays. Figure 2(b) shows the multiplicity distribution of charged hadrons for $\sqrt{s} = 14$ and 34.5 GeV. At 14 GeV we see an almost perfect agreement between theory and calculation; at 34.5 GeV the measured multiplicity distribution is narrower than the calculated one. This is a first hint that the 34.5-GeV data show more than phase space.

Figure 3 displays the transverse-momentum distribution at $\sqrt{s} = 14$ and 34.5 GeV. For each energy we present the transverse-momentum distribution of all charged particles as well as the average squared transverse momentum as a function of Feynman x. For 14 GeV we observe an almost complete agreement between theory and experiment for the p_T distribution of all particles as well as for $\langle p_T^2 \rangle(x)$. Since our fragmentation is completely symmetric for both jets we can conclude that the asymmetry of the "seagull" shape of $\langle p_T^2 \rangle(x)$ at this energy is completely due to the sphericity analysis. Because of the fluctuations of the momentum of the charged particles it produces always a wide and a narrow jet. At

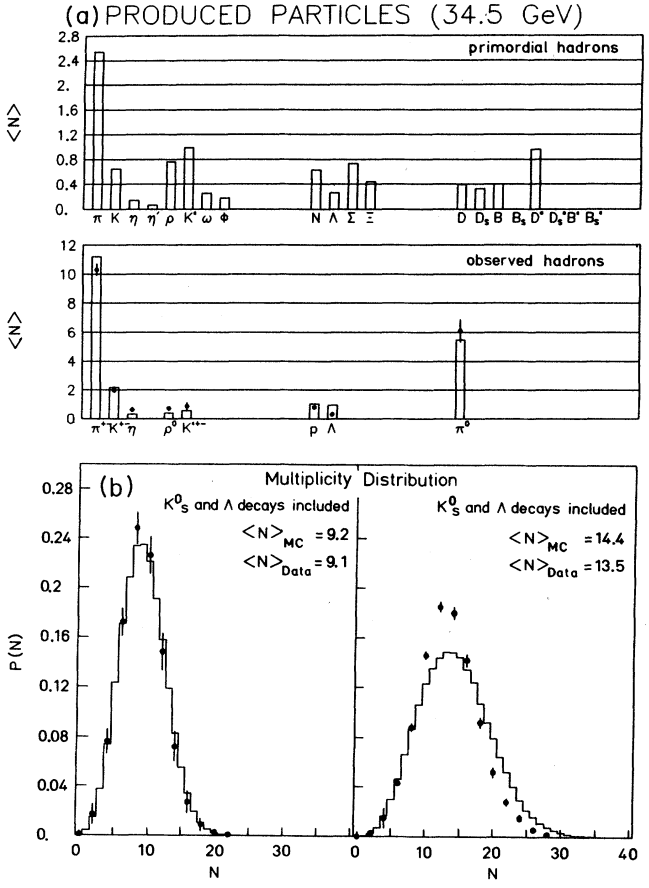

FIG. 2. Multiplicities. (a) The mean multiplicities of primordial and observed particles at 34.5 GeV. (b) Multiplicity distributions for charged particles at 14 and 34.5 GeV.

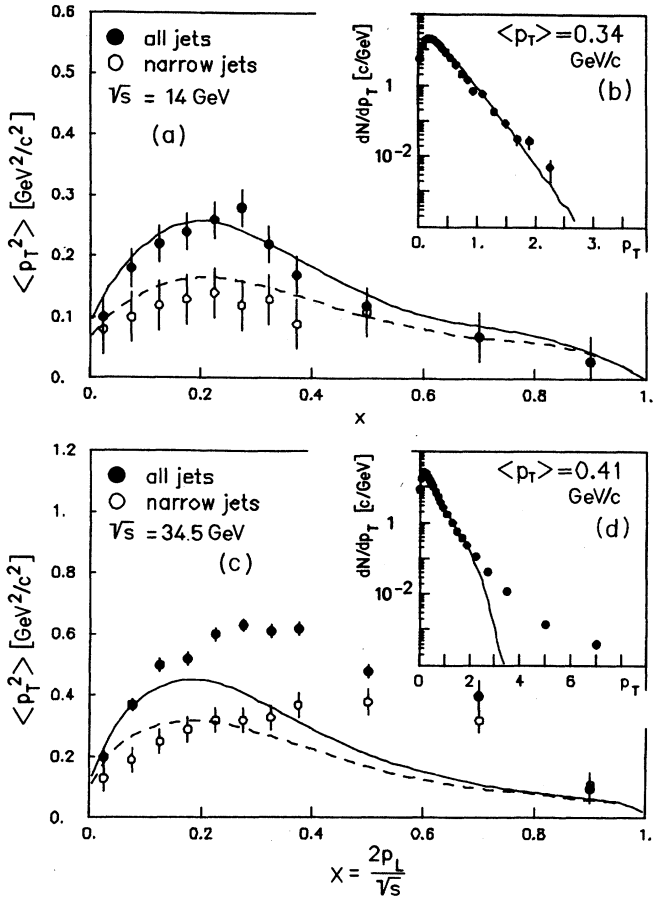

FIG. 3. Transverse momenta. (b) and (d) Distribution of transverse momentum p_T with respect to the sphericity axis. (a) and (c) Average squared transverse momentum $\langle p_T^2 \rangle$ as a function of x_L for charged particles at 14 and 34.5 GeV.

34.5 GeV we still see an agreement between theory and data over 2 orders of magnitude for the p_T distribution. This distribution is determined by the low-x particles. At large x we see some differences. There the theoretical $\langle p_T^2 \rangle(x)$ is considerably smaller than the experimental one. Obviously three-jet events, which are not included in our analysis, become important at 34.5 GeV. This, however, is the only place in the analysis where the phase-space approach is insufficient to explain the data quantitatively.

We have seen that the majority of available e^+e^- data at various energies can be well described assuming a sequential decay of a string into hadrons. Each step is described by Fermi's golden rule assuming that the matrix elements are dependent on the transverse momentum only and the longitudinal distribution is completely determined by phase space. The only parameter employed in this approach is $\langle p_T^2 \rangle$. Consequently, single-particle-inclusive fragmentation data reveal little about the underlying QCD mechanism. It seems that the numerous adjustable parameters of the more complicated fragmentation models cancel because longitudinal phase space only describes the data on the same level of agreement.

This work has been funded in part by the German Federal Minister for Research and Technology (BMFT) under Contract No. 06HD776 and by the Gesellschaft für Schwerionenforschung (GSI).

[1]R. Baier, J. Engels, H. Satz, and K. Schilling, Nuovo Cimento **28**, 455 (1975); L. van Hove, Nucl. Phys. **B9**, 331 (1969).
[2]R. D. Field and R. P. Feynman, Nucl. Phys. **B136**, 1 (1978).
[3]B. Andersson *et al.*, Phys. Rep. **97**, 31 (1983).
[4]B. R. Webber, Nucl. Phys. **B238**, 492 (1984).
[5]Y. Kurihara, J. Hüfner, and J. Aichelin, Phys. Lett. B **205**, 549 (1988).
[6]TASSO Collaboration, M. Althoff *et al.*, Z. Phys. C **22**, 307 (1984); **17**, 5 (1983); B. Naroska, Phys. Rep. **148**, 67 (1987).